# Thermal-magneto-mechanical stability analysis of single-walled carbon nanotube conveying pulsating viscous fluid

R. Selvamani[*1], M. Mahaveer Sree Jayan[2] and Marin Marin[3]

[1]*Department of Mathematics, Karunya University, Coimbatore, 641 114, Tamil Nadu, India*
[2]*Department of Mathematics, Indra Ganesan College of Engineering, Tiruchirappalli, 620012, Tamilnadu, India*
[3]*Department of Mathematics and Computer Science, Transilvania University of Brasov, Romania*

**Abstract.** In this study, the vibration problem of thermo elastic carbon nanotubes conveying pulsating viscous nano fluid subjected to a longitudinal magnetic field is investigated via Euler-Bernoulli beam model. The controlling partial differential equation of motion is arrived by adopting Eringen's non local theory. The instability domain and pulsation frequency of the CNT is obtained through the Galerkin's method. The numerical evaluation of this study is devised by Haar wavelet method (HWM). Then, the proposed model is validated by analyzing the critical buckling load computed in present study with the literature. Finally, the numerical calculation of system parameters are shown as dispersion graphs and tables over non local parameter, magnetic flux, temperature difference, Knudsen number and viscous parameter.

**Keywords:** dynamic stability; Haar wavelet method; Knudsen number; nonlocal parameter; pulsating nano flow; viscous fluid

## 1. Introduction

The coupling effect of fluid and nano structures has been received more and more research and physical construction interest to engineers in order to acquire the interactive mechanical behaviour of this system. Fluid will not expose the actual speed while it is passing through the pipe owing to power systems changes. Thus, the pattern of flow becomes pulsatile inward through the pipe and the tube experience the pulsatile nature too and dynamic character of such type may be the efficient idea to handle this phenomenon. Nonlocal elasticity, as a prevalent size dependent phenomenon, has been presented by (Eringen 1983, Eringen and Edelen 1972). Fluid conveying nano systems via continuum based analysis has received much attention in recent years (Lee 2008, Wang 2009, Ghavanloo and Fazelzadeh 2011, Zhen *et al.* 2011, Wang *et al.* 2008, Kuang *et al.* 2009, Ghavanloo *et al.* 2011). Both viscous and elastic character is being exposed by viscoelastic materials. These type of component will be very chaotic in mechanical waves via damping property. There are many models to describe the viscoelastic behaviour such as Maxwell (Xia and

---

∗Corresponding author, Ph.D., E-mail: selvam1729@gmail.com

Wang 2010, Rashidi *et al.* 2012, Hosseini and Sadeghi-Goughari 2016, Li *et al.* 2016, Karlicic*et al.* 2017, Murmu *et al.* 2012). The propulsion of magnetic field variants will have center of attention in drug delivery through short time and efficient waver by changing its intensity (Given 2014, Kiani 2014, Kiani 2015, Zhang *et al.* 2006, Liu *et al.* 2018, Ibrahimbegovic *et al.* 2022, Hajdo *et al.* 2021, Nguyen *et al.* 2022, Ibrahimbegovic and Mejia-Nava 2021) investigated the effect of nano flow on vibration of nanotube conveying fluid using Knudsen and Knudsen-dependent flow velocity on vibrations of a nanotube conveying fluid. They used Euler–Bernoulli plug-flow beam theory and modified no-slip condition of nanotube conveying fluid based on Kn (Knudsen number). Also, they considered the effect of slip condition, for a liquid and a gas flow.

The energy and fastness of the particles is highly motivated by temperature growth. This type of method has been discussed vividly by many scientists (Raravikar *et al.* 2002, Schelling Keblinski 2003, Pipes and Hubert 2003, Zhang and wang 2005, Ni *et al.* 2002, Zhang and Shen 2006. Zhang *et al.*2007). Paidoussis and Sundararajan (1975) conducted a dynamic survey on pulsating fluid conveying pipe via Bolotin's and Floquet analysis. The analytical model of stability checking and support stimulation of PFCP (Pulsating Fluid Conveying Pipe) was constructed by Ariaratnam and Namachchivaya (1986). Noah and Hopkins (1980) carried out dynamic study of PFCP to expose the effect of flexibility on steady and pulsating waves. Jin and Song (2005) performed the physical parameter analysis on supported PFCP via numerical calculations and interpretations. Employing the internal resonance of the system, (Panda and Kar 2007, Panda and Kar 2008). Conducted a nonlinear bending analysis in a pinned–pinned PFCP in the frame of principal parametric resonance. Incorporating algorithm of fourth-order Runge–Kutta method, Ni *et al.* (2014) adopted coupled PFCP to verify the nonlinear bending characteristics. Again, owing to showcase the in and out plane pulsation frequency of curved PFCP, vibration studies were conducted by Ni *et al.* (2014). Zhang *et al.* (2017) carried out a dynamical survey and perturbation detail in multi-pulse dynamics of the cantilevered PFCP. Herein the principal of parametric resonance was taken in to account.

Nowadays, differential and integro-differential equations conveniently solved by Haar wavelets method. The Haar wavelets are generated from pairs of piecewise constant functions and can be simply integrated. Furthermore, the Haar functions are orthogonal and it forms a good transform basis. Chen and Hsiao (1997) evaluated lumped and distributed system parameters via Haar wavelet method. The Haar wavelet method has been adjusted for solving wide class of differential and integral equations which are covering solid and fluid mechanics (Hein and Feklistova 2011), mathematical physical problems (Heydari *et al.* 2014, Hsiao 2015, Jin *et al.* 2014). The validity and accuracy of HWM was elaborated vividly and also evaluated analytically via shear
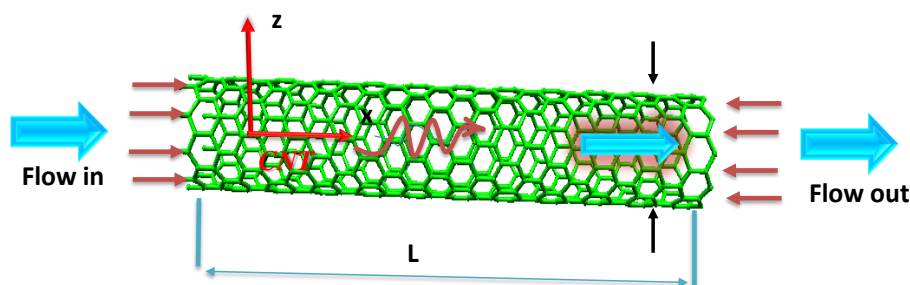


Fig. 1 A PFC SWCNT with longitudinal magnetic load

deformation theory (Jena and Chakravarty 2019, Lepik and Estonian 2011, Jena *et al.* 2019). Literature review reveals the lack of availability of an analytical investigation concerning with, the vibration problem of thermo elastic pulsed viscous fluid conveying carbon nanotubes subjected to a longitudinal magnetic field via Haar wavelet theory. Thus, the authors aimed to construct an analytical model of the vibration problem of thermo elastic carbon nanotubes conveying pulsating viscous nano fluid stimulated by magnetic field through longitudinal axis via Haar wavelet method and a set of numerical examples are presented to showcase how each of the variant influences the viscous fluid conveying nanotube structure's endurance.

## 2. Mathematical formulation

### 2.1 Erigen nonlocal continuum theory

The relationship for linear, homogeneous, isotropic and non-local elastic with body forces are defined in constitutive form by (Eringen 1983) as

$$\Pi_{ij} + \rho(f_j - \ddot{u}_j) = 0, \tag{1}$$

$$\Pi_{ij}(x) = \int_v \pi(|x - x'|), \tau)\Pi_{ij}{}^c(x')dV(x'), \tag{2}$$

$$\Pi_{ij}{}^c = C_{ijkl}\varepsilon_{kl}. \tag{3}$$

$$e_{ij}(x') = \frac{1}{2}\left(\frac{\partial u_i(x)}{\partial x_{j'}} + \frac{\partial u_i(x')}{\partial x_{j'}}\right). \tag{4}$$

where $\Pi_{ij,i}, \rho, f_j, u_j$ are the stress tensor, density, body force and displacement vector at a reference point $x$ in the body via the time $t$, where $\Pi^c{}_{ij}(x')$ is the classical stress tensor at any point $x'$ in the body, which is related to the linear strain tensor $e_{ij}(x')$. The kernel function which will add nonlocal effect in the relation is represented by $\pi(|x - x'|, \tau)$ is the nonlocal attenuation function at $x$ which is created by the local strain at $x'$. Eq. (2) denotes the volume integral over the region of the body $v$. With the internal and external characteristic length $a$ and $l$, respectively, the attenuation function has the form

$$\pi(|x - x'|, \tau), \tau = \frac{e_o a}{l}. \tag{5}$$

The material constant $e_0$ is to be found for each and every material and "$|x - x'|$" is the Euclidian distance. Further, Eq. (2) is rewritten as

$$(1 - \tau^2 l^2 \nabla^2)\Pi_{ij}(x) = \Pi_{ij}{}^c(x) = C_{ijkl}e_{kl}(x), \tag{6}$$

where $C_{ijkl}$ is the elastic modulus tensor and $e_{ij}$ is the strain tensor. Where $\nabla^2$ denotes the second-order spatial gradient applied on the stress tensor $\Pi_{ij}$ and $\tau = e_o a/l$. Eringen exposed $e_o = 0.39$ by the matching of the dispersion curves via non-local theory for place wave and born-Karman model of lattice dynamics at the end of the Brillouin zone $(ka = \pi)$, where $a$ is the distance between atoms and $k$ is the wave number in the phonon analysis.

## 3. Basic formulation

The classical controlling equations of fluid conveying CNT which poses the force term,

magnetic field, thermal load, fluid flow can be designed via Euler-Bernoulli beam in the partial form as

$$\frac{\partial S}{\partial x} + N_t \frac{\partial^2 y}{\partial x^2} - \frac{\partial y}{\partial t}\left[C + \rho A \frac{\partial y}{\partial t}\right] + q_z \frac{\partial^2 y}{\partial x^2} + F_p + F_m = m_c \frac{\partial^2 y}{\partial t^2}, \qquad (7)$$

where $S$, $F_p$ and $F_m$ represents the shear force, fluid flow force and the longitudinal magnetic field force, respectively. The transverse force $S$ and moment of bending $M$ of viscoelastic tube via Euler-Bernoulli beam model is reached as (Paidoussis 1998)

$$S = \frac{\partial M}{\partial X} = \left(E - C\frac{\partial}{\partial t}\right)I\frac{\partial^3 y}{\partial x^3}. \qquad (8)$$

the thermal loading force $N_t$ is arrived as

$$N_t = \frac{EA\alpha_x T}{(1-2v)}\frac{\partial^2 y}{\partial x^2}. \qquad (9)$$

Here in $E$, $A$, $v$, $\alpha_x$ and $T$ are the Young modulus, tube cross section, poison ratio of the CNT, thermal expansion and the temperature changes respectively. The Lorentz force induced longitudinal magnetic flux $q_Z$ (Selvamani *et al.* 2020)

$$q_z = \eta A H_x^{\ 2}\frac{\partial^2 y}{\partial x^2}. \qquad (10)$$

The viscos-fluid flow force on the CNT is achieved as (Mahaveer Sree Jayan *et al.* 2020) (Amiri *et al.* 2018)

$$F_p = m_f\left(2U_x\frac{\partial^2 y}{\partial x\partial t} + U_x^{\ 2}\frac{\partial^2 y}{\partial x^2} + \frac{\partial^2 y}{\partial t^2}\right) + \left(\mu_e A_f \frac{\partial^2 y}{\partial x^2}\left(\frac{\partial y}{\partial x\partial t} + U_x\frac{\partial y}{\partial x}\right)\right). \qquad (11a)$$

here $m_f$, $U_x$, $A_f$ and $\mu_e$ are the fluid mass, fluid viscosity possessing slip boundary condition, fluid flow cross section and modified viscosity, respectively. Modified fluid velocity $\mu_e$ and fluid bulk viscosity $\mu_0$ via the rarefaction coefficient $C_r(Kn) = \frac{1}{(1+\alpha Kn)}$ is taken as

$$\mu_e(Kn) = \mu_0 \frac{1}{(1+\alpha Kn)}. \qquad (11b)$$

herein $(Kn)$ is the Knudsen number and $\alpha$ is defined as

$$\alpha = \frac{2}{\pi}\alpha_0[\tan^{-1}(\alpha_1 Kn^R)]. \qquad (11c)$$

Where the values of $\alpha_1$ and $R$ is assumed as 4 and 0.4, respectively and $\alpha_0$ is

$$\lim_{kn\to\infty}\alpha = \alpha_0 = \left(\frac{64}{3\pi\left(1-\frac{4}{b}\right)}\right). \qquad (11d)$$

the parameter $b$ is set to be -1 for the case of slip boundary. Owing to use slip boundary condition, the velocity correction factor VCF is adopted as

$$VCF = \frac{U_x}{U_{x(no-slip)}} = \frac{1}{C_r(Kn)}\left(4\left(\frac{2-\sigma_v}{\sigma_v}\right)\right)\left(\frac{Kn}{(1+\alpha Kn)}\right) + 1. \qquad (11e)$$

The magnitude of $F_m$ is considered as in (Azrar *et al.* 2015)

$$F_m = M_f\frac{\partial U_x}{\partial t}(L-x)\left(\frac{\partial^2 y}{\partial x^2}\right). \qquad (12)$$

Where $L$ is length of the tube and bending stiffness $EI$ can be modified as (Lei *et al.* 2012)

$$EI^* = EI + Q_s E_s, \tag{13}$$

here $Q_s = \frac{\pi}{8}(d + h)^3$ and $E_s$ is the Young's modulus of surface and $h$ is the effective thickness of SWCNTs, respectively and the diameter is $d = \frac{3na}{\pi}$ (Li *et al.* 2016). As per bending moment $M$ which is in Eq. (8) takes the form as

$$M = \int_A z\, \Pi_{xx}\, dA, \tag{14}$$

According to Eq. (6), the non-local form of 1-D nanotube is taken as

$$\Pi_{xx} - (e_0 a)^2 \frac{\partial^2 \Pi_{xx}}{\partial x^2} = E e_{xx}, \tag{15}$$

where $e_{xx}$ is the strain in axial mode, $(e_0 a)$ is a nonlocal parameter. Eq. (15) is rewritten via temperature terms as

$$\Pi_{xx}\left(1 - (e_0 a)^2 \frac{\partial^2}{\partial x^2}\right) = E(e_{xx} - \alpha T). \tag{16}$$

Where $e_{xx}$ through small bending model is showcased as

$$e_{xx} = -z \frac{\partial^2 y}{\partial x^2}, \tag{17}$$

By employing Eq. (16) and (17) in to Eq. (14) gives

$$M\left(1 - (e_0 a)^2 \frac{\partial^2}{\partial x^2}\right) = EI^* \frac{\partial^2 y}{\partial x^2}, \tag{18}$$

By substituting Eq. (14) into Eq. (18) leads to

$$M - (e_0 a)^2 \left[(\rho A)\frac{\partial^2 y}{\partial t^2} + q_z - f(x) + EA\alpha T\right] = EI^* \frac{\partial^2 y}{\partial x^2}.$$

$$S - (e_0 a)^2 \left[(\rho A)\frac{\partial^3 y}{\partial x^2 \partial t^2} + \frac{\partial^2 q_z}{\partial x^2} - \frac{\partial f(x)}{\partial x} + EA\alpha T\right] = EI^* \frac{\partial^3 y}{\partial x^3}. \tag{20}$$

According to Eq. (7), motion equation takes the form

$$\left(1 + C\frac{\partial y}{\partial t}\right)EI\frac{\partial^4 y}{\partial x^4} + \begin{bmatrix} EA\alpha T - R + \rho A(1 - 2v) + \\ M_f \frac{\partial U_x}{\partial t}(L - x) - \eta_s A H_x^2 \frac{\partial^2 y}{\partial x^2} + M_f U_x^2 \end{bmatrix}\frac{\partial^2 y}{\partial x^2} +$$

$$(m + M_f)\frac{\partial^2 y}{\partial t^2} + 2m_f U_x \frac{\partial^2 y}{\partial x \partial t} + rA\left(U_x \frac{\partial^2 y}{\partial x^3} + \frac{\partial^2 y}{\partial x^2 \partial t}\right) -$$

$$(\tau)^2 \begin{pmatrix} EA\alpha T \frac{\partial^4 y}{\partial x^4} + m\frac{\partial^2 y}{\partial x^2 \partial t^2} + M_f \frac{\partial^2 y}{\partial x \partial t} + M_f U_x^2 \frac{\partial^4 y}{\partial x^4} \\ + 2M_f U_x \frac{\partial^4 y}{\partial x^2 \partial t} - \eta_s A H_x^2 \frac{\partial^4 y}{\partial x^4} \end{pmatrix} = 0. \tag{21}$$

Using Eq. (11e) into Eq. (21) poses

$$\left(1 + C\frac{\partial y}{\partial t}\right)EI\frac{\partial^4 y}{\partial x^4} +$$

$$\left[\begin{array}{l} EA\alpha T - R + \rho A(1-2v) + M_f\,\dfrac{\partial U_x avg(slip)}{\partial t}(L-x) - \\[2mm] \eta_s AH_x{}^2\dfrac{\partial^2 y}{\partial x^2} + M_f(VCF)U_x{}^2avg(slip) \end{array}\right]\dfrac{\partial^2 y}{\partial x^2} +$$

$$(m+M_f)\dfrac{\partial^2 y}{\partial t^2} + 2m_f(VCF)U_x avg(slip)\dfrac{\partial^2 y}{\partial x \partial t} +$$

$$rA\left(U_x avg(slip)\dfrac{\partial^2 y}{\partial x^2} + \dfrac{\partial^3 y}{\partial x^2 \partial t}\right) -$$

$$(\tau)^2\left(\begin{array}{l} EA\alpha T\dfrac{\partial^4 y}{\partial x^4} + m\dfrac{\partial^4 y}{\partial x^2 \partial t^2} + M_f\dfrac{\partial^4 y}{\partial x^2 \partial t^2} + \\[2mm] M_f(VCF)U_x{}^2avg(slip)\dfrac{\partial^4 y}{\partial x^4} \\[2mm] +2M_f(VCF)U_x avg(slip)\dfrac{\partial^4 y}{\partial x^3 \partial t} - \eta_s AH_x{}^2\dfrac{\partial^4 y}{\partial x^4} \end{array}\right) = 0. \qquad (22)$$

the following dimensionless quantities are determined for simple calculation

$$\dfrac{x}{L} = \xi, \dfrac{y}{L} = \eta, \delta = \left(\dfrac{EI^*}{M_f+m}\right)^{\frac{1}{2}}\dfrac{t}{L^2}, \tau = \dfrac{e_0 a}{l}, u = \left(\dfrac{M_f}{EI^*}\right)^{\frac{1}{2}}LU_x, \gamma = \left(\dfrac{EI^*}{M_f+m}\right)^{\frac{1}{2}}\dfrac{C}{L^2}, T = \dfrac{NL^2}{EI^*} - \dfrac{\rho AL^2}{EI^*}(1 -$$

$$2v), \beta = \dfrac{\gamma A}{\sqrt{EI^*M_f}}, M_r = \left(\dfrac{M}{M_f+m}\right)^{\frac{1}{2}}, \bar{N}_T = \dfrac{N_T L^2}{EI^*}, M_q = \dfrac{\eta AH_x{}^2 L^2}{EI^*}.$$

Hence, Eq. (22) in non-dimensional form

$$\gamma \overset{*}{\xi}{}^{//} + \xi^{//} + \left[u^2 + N_t - T - M_q + M_r\overset{*}{u}(1-\eta)\right]\xi^{//} + \overset{**}{\xi} + 2M_r u\overset{*}{\xi}{}^{//} - \beta\left(u\xi^{//} + M_r\overset{*}{\xi}{}^{//}\right) -$$

$$\tau^2\left(\overset{*}{\xi}{}^{//} + u^2\xi^{//} + N_t\xi^{//} - M_q\xi^{//} + 2M_r u\overset{*}{\xi}{}^{//}\right) = 0. \qquad (23)$$

Where $( )^{/} = \dfrac{\partial()^{/}}{\partial \eta}, ( )^* = \dfrac{\partial()^{/}}{\partial \delta}$. The internal pulsating axial flow is taken in to the account and the flow velocity under harmonically undulate form is as (Azrar 2015)

$$u = u_o[1 + \Psi \cos(\Omega t)]. \qquad (24)$$

where $u_0$ is the mean flow velocity, $\Psi$ is the amplitude of the harmonic undulation and $\Omega$ its frequency. Galerkin method is adopted to detach Eq. (24) as

$$\eta(\xi,\delta) = \sum_{i=1}^{2}\chi_i(\xi)\,\varphi_i(\delta), \qquad (25)$$

here $\chi_i(\eta), \varphi_i(\delta)(i = 1,2.,,,,,,,)$ are explains the eigen functions corresponding to clamped side and in generalized terms of coordinates. By relaying Eqs. (24) and (25) into Eq. (23) results the characteristics of orthogonal mode shapes via first order 4-dimensional differential equations as

$$\dot{k} = Bk + \psi\,\Omega\,P_1 k\sin(\Omega\delta) - \psi\,\Omega\,P_2 k\cos(\Omega\delta) - \gamma P_3 k. \qquad (26)$$

where $k = [k_1, k_2, k_3, k_4]^T, k_3, = \dot{k_1}, \ \dot{k_4} = k_2, \ \gamma = \psi\bar{\gamma},$

## 4. Fundamentals of Haar wavelet theory

The Haar function can be defined as

$$
h_i(t) = \begin{cases} 1, & for \quad t \in [\xi_1(i), \xi_2(i)], \\ -1, & for \quad t \in [\xi_2(i), \xi_3(i)], \\ 0, & \quad\quad otherwise, \end{cases} \tag{27a}
$$

where the higher magnitude of square waves $i = m + k + 1$, $m = 2^j$ which belongs to $[X, Y]$, $k$ is the specific square wave point. So, we have the following terms in the interval $[X, Y]$ (Jena and Chakraverty 2019) (Lepik and Estonian 2011)

$$
\xi_1(i) = X + k \frac{Y - X}{2^j},
$$

$$
\xi_2(i) = X + (2k + 1) \frac{Y - X}{2^{j+1}},
$$

$$
\xi_3(i) = X + (k + 1) \frac{Y - X}{2^j}. \tag{27b}
$$

where $j$ and $k$ are known as the wavelet's dilatation and translation, respectively $j = 0,1,2.,\dots J$ and $k = 0,1,\dots, 2^J - 1$. where $J$ is maximum resolution level of wavelets. Eq. (27a) is valid for $i > 2$. For $i = 1, h_i(t) = 1$ for $t \in [X, Y]$ and 0 in the rest. Every function $\varphi(t) \in [X, Y]$ which is square integrable and finite has the form via Haar wavelet as

$$
\phi(t) = \sum_{t=1}^{2^{j+1}} a_i h_i(t). \tag{27c}
$$

Hence Eq. (27a) read as

$$
P_{n,i}(t) = \begin{cases} 0, & for \quad t \in [X, \xi_q(i)), \\ (t - \xi_q(i)^n, & for \quad t \in [\xi_q(i), (\xi_2(i))), \\ (t - (\xi_q(i))^n - 2(t - (\xi_2(i))^n, & for \quad t \in [\xi_2(i), (\xi_3(i)), \\ (t - (\xi_q(i))^n - 2(t - (\xi_2(i))^n + t - (\xi_3(i))^n, & for \quad t \in [\xi_3(i), Y). \end{cases} \tag{27d}
$$

Eq. (27d) is valid for $i > 1$. For $i = 1$ , $\xi_1 = X, \xi_2 = \xi_3 = Y$ and

$$
P_{n,i}(t) = \frac{1}{n!} (t - X)^n, \tag{27e}
$$

herein collocation points are developed as

$$
t_k = A + (k - 0.5) \frac{Y - X}{2^{J+1}}, \rightleftarrows\rightleftarrows k = 1,2,\dots\dots\dots 2^{J+1}. \tag{27f}
$$

where $H, P_1, P_2, P_3, P_4, \dots\dots P_n$ are Haar square with dimension $2^{J+1}$ and the components in this matrices are evaluated as $H(i, k) = H_t(t_k)$ and $P_n(i, k) = p_{n,t}(t_k)$.

### 4.1 Haar wavelet method

As in Haar wavelet theory, the highest-order derivative in Eq. (22) can be modelled as (Jena and Chakraverty 2019):

$$
\frac{\partial^4 y}{\partial x^4} = \sum_{i=1}^{2^{J+1}} c_i h_i = c^T H, \tag{28a}
$$

Through four time successive integration

$$\frac{\partial^2 y}{\partial x^2}(x) = \sum_{i=1}^{2^{J+1}} c_i P_{2,i}(x) + x\frac{\partial^3 y}{\partial x^3}(0) + \frac{\partial^2 y}{\partial x^2}, \tag{28b}$$

$$\frac{\partial^2 y}{\partial x^2}(x) = \sum_{i=1}^{2^{J+1}} c_i P_{2,i}(x) + x\frac{\partial^3 y}{\partial x^3}(0) + \frac{\partial^2 y}{\partial x^2}, \tag{28c}$$

$$\frac{\partial y}{\partial x}(x) = \sum_{i=1}^{2^{J+1}} c_i P_{3,i}(x) + \frac{x^2}{2}x\frac{\partial^3 y}{\partial x^3}(0) + \frac{\partial y}{\partial x}(0), \tag{28d}$$

$$y(x) = \sum_{i=1}^{2^{J+1}} c_i P_{4,i}(x) + \frac{x^3}{6}\frac{\partial^3 y}{\partial x^3}(0) + \frac{x^2}{2}\frac{\partial^2 y}{\partial x^2}(0) + x\frac{\partial y}{\partial x}(0) + y(0). \tag{28e}$$

here $\quad C = (c_1, c_2, c_3, c_4 \ldots \ldots \ldots c_{2^{J+1}})^T \quad$ and $\quad D = \left( \left(d_1 = \frac{\partial^3 y}{\partial x^3}(0)\right), \left(d_2 = \frac{\partial^2 y}{\partial x^2}(0)\right), \right.$

$\left. \left(d_3 = \frac{\partial y}{\partial x}(0)\right), (d_4 = y(0)) \right)^T$ The constant of integration $d_1, d_3, d_3$ and $d_4$ can be reached via specific boundary conditions

Inserting Eq. (28a)-(28e) in controlling Eq. (22), we arrived as

$$\left(1 + C\frac{\partial y}{\partial t}\right)C^T H + \begin{bmatrix} EA\alpha T - R + \rho A(1-2v) + M_f \dfrac{\partial U_x avg(slip)}{\partial t}(L-x) - \\ \eta_s AH_x{}^2 + M_f(VCF)U_x{}^2 avg(slip) \end{bmatrix}(C^T p_2 + xd_1 + d_1)$$

$$+ (m + M_f)\frac{\partial^2 y}{\partial t^2} + \frac{\partial}{\partial t}\left(2m_f(VCF)U_x avg(slip)\right)(C^T p_3 + \frac{x^2}{2}d_1 + xd_{2+}d_3) +$$

$$\left(rAU_x avg(slip)(C^T p_2 + xd_1 + d_1)\frac{\partial^2 y}{\partial x^2} + \frac{\partial}{\partial t}rA\left((C^T p_2 + xd_1 + d_1)\right)\right) - (\tau)^2$$

$$\begin{pmatrix} (EA\alpha T)C^T H + \frac{\partial^2 y}{\partial t^2}m((C^T p_2 + xd_1 + d_1)) + M_f(C^T p_2 + xd_1 + d_1)\frac{\partial^2 y}{\partial t^2} + \\ \left(M_f(VCF)U_x{}^2 avg(slip)\right)C^T H \rightleftharpoons + \frac{\partial}{\partial t}2M_f(VCF)U_x avg(slip)\left(C^T p_3 + \frac{x^2}{2}d_1 + xd_{2+}d_3\right) \\ -(\eta_s AH_x{}^2)C^T H \end{pmatrix} = 0. \tag{29}$$

Herein, the following boundary conditions are taken for numerical calculations

(i). $\; y(0) = 0, \frac{\partial^2 y}{\partial x^2}(0) = 0$ and $y(L) = 0, \frac{\partial^2 y}{\partial x^2}(L) = 0,$ Hinged-Hinged (H-H).

(ii). $\; y(0) = 0, \frac{\partial y}{\partial x}(0) = 0$ and $y(L) = 0, \frac{\partial^2 y}{\partial x^2}(L) = 0,$ Clamped-Hinged (C-H).

(iii). $\; y(0) = 0, \frac{\partial y}{\partial x}(0) = 0$ and $y(L) = 0, \frac{\partial y}{\partial x}(L) = 0,$ Clamped–Clamped (C-C).

(iv). $\; y(0) = 0, \frac{\partial y}{\partial x}(0) = 0$ and $\frac{\partial^2 y}{\partial x^2}(L) = 0, \frac{\partial^3 y}{\partial x^3}(L) = 0.$ Clamped – Free (C-F).

By using each of the particular boundary condition as mentioned above, the integration constants $D^T = (d_1, d_3, d_3, d_4)$ can be determined and using these values in Eq. (29), then we can receive a generalized Eigenvalue problem as

$$[A]\{C^T\} = \tau^2[B]\{C^T\}. \tag{30}$$

Where the matrix $[A]$ represents mass and the matrix $[B]$ is for stiffness and $C^T =$

$(c_1, c_3, c_3, c_4 \ldots \ldots c_{2J+1})$.

## 5. Results and discussion

The obtained variants are allocated and verified numerically to expose the scientific importance of various parameters on the stability of SWCNT with viscous fluid conveying environment. The nonlocal and viscous parameters, Knudsen number, magnetic flux, temperature difference and boundary influence on the dynamics of CNT are analysed and verified via tables and dispersion graphs. The physical constants taken for this study is given in (Table1).

The excitation frequency of non-dimensional form is presented as below

Table 1 Material properties (Lee and Chang 2008, Li *et al.* 2016)

| Parameters | Value |
|---|---|
| $EI$ | $1.1122 \times 10^{-25}$ N m$^9$ |
| $\alpha^0$ | $-1.5 \times 10^{-6}$ C$^{-1}$ |
| $\rho$ | 2.3 g/cm$^3$ |
| $e_0$ | 0.31 nm |
| $a$ | 0.142 N/m |
| $E_s$ | 35.3 N/m |
| $\mu$ | $4\pi \times 10^{-7}$ N/m |
| $H_x$ A/m | $2 \times 10^8$ A/m |
| $\sigma$ | $1.02 \times 10^6$ (s/m) |
| $\tau d$ | 0 s |
| $u_0$ | 2.0 |
| $\gamma$ | 0.001 |
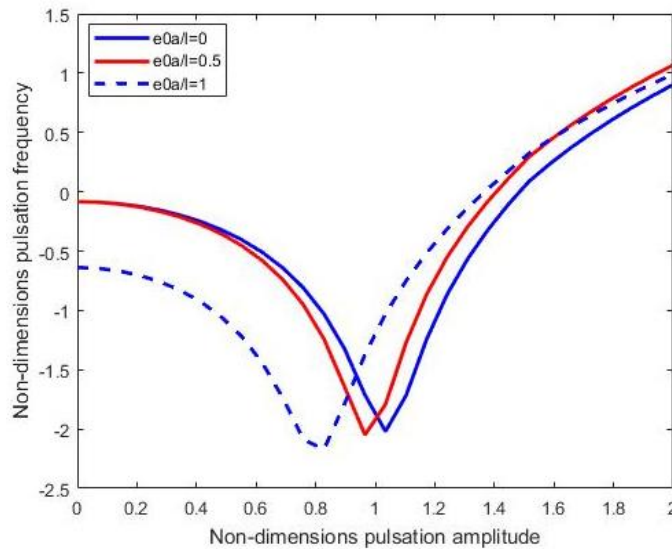


Fig. 2 Distributions of nondimentional pulsation frequency versus nondimensional pulsation amplitude via different nonlocal parameter with $\beta = 0.3$
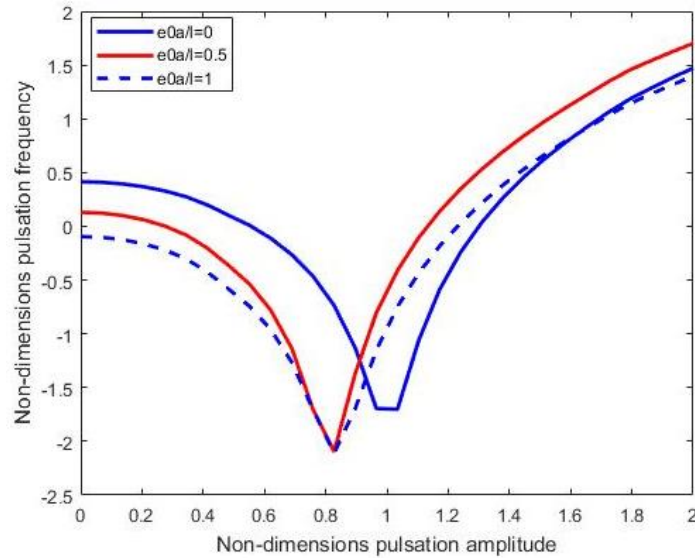
Fig. 3 Distributions of nondimentional pulsation frequency versus nondimensions pulsation amplitude via different nonlocal parameter with $\beta = 0.5$

Table 2 Verification of critical buckling load parameter by HWM with Jana and Chakraverty (2019) ($e_0 a = 0.5$, $k_w = 0$, $H_a = 2$ $\beta = 0.2$, $K_n = 0.1$ and $L = 20$) via Hinged boundary condition

|  |  | Jana and Chakraverty (2019) | Present |
|---|---|---|---|
| $J$ | $N = 2^{J+1}$ | $HWM$ | $HWM$ |
| 1. | 4 | 2.314765 | 2.3145 |
| 2. | 8 | 2.303851 | 2.3013 |
| 3. | 16 | 2.301451 | 2.3012 |
| 4. | 32 | 2.300871 | 2.3011 |
| 5. | 64 | 2.300728 | 2.3009 |
| 6. | 128 | 2.300692 | 2.3008 |
| 7. | 256 | 2.300683 | 2.3004 |
| 8. | 512 | 2.300681 | 2.2983 |

$$\Omega = \omega_{ex} L^2 \left( \frac{\rho_1 A}{E_1 I} \right)^{0.5}$$

The present study is validated in Table 1 through the critical buckling load by Haar wavelet method via $e_0 = 0.5$, $e_0 a = .5$, $H_x = 0.2$, $\beta = 0.2$, $K_n = 0.1$ and $L = 20$ for Hinged-Hinged boundary condition with article in the literature (Jena *et al.* 2019). Results predict the reasonable agreement with the literature. Table 2 exhibit the convergence of mean flow velocity, viscous parameter and different boundary conditions on the non-dimensional pulsation frequency via $J = 1 - 5$. From Table 2, it is seen that the frequencies are increasing for the amplified values of mean flow velocity, viscous parameter and decreasing with increasing maximal resolution values($J$). This leads to the conclusion that the stability of the fluid conveying CNT structure becomes weak by rising the resolution values while increase the flow velocity, viscous parameter the dynamic
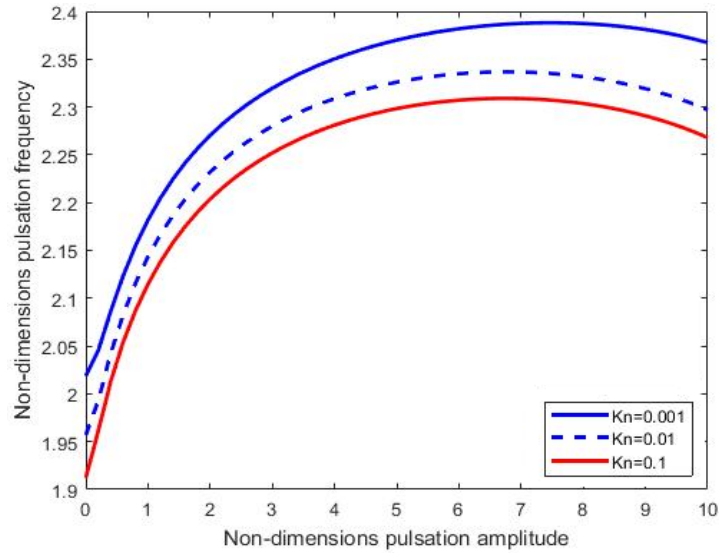
Fig. 4 Distributions of nondimentional pulsation frequency versus nondimensional pulsation amplitude via different Knudsen number with $\beta = 0.3$
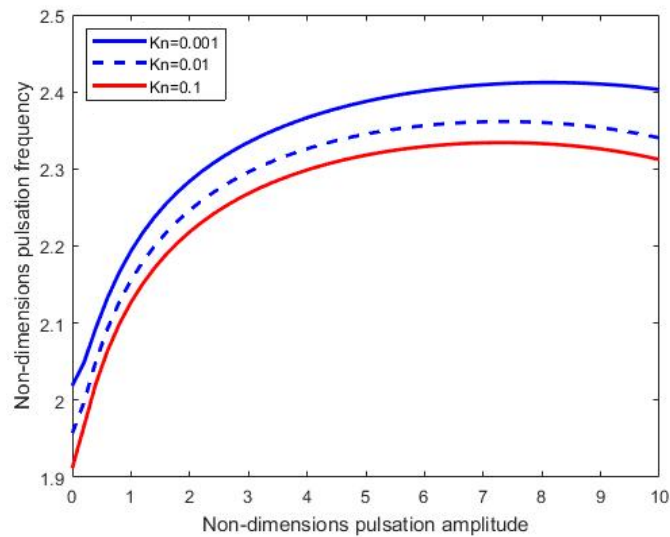


Fig. 5 Distributions of nondimentional pulsation frequency versus nondimensional pulsation amplitude via different Knudsen number with $\beta = 0.5$

behaviour of the system develops. Among the boundary conditions, the C-C boundary reached higher pulsation frequency than the other three boundaries.

Figs. 2 and 3 presents to study the development of non-dimensional pulsation frequency of fluid conveying CNT with non-dimensional pulsation amplitude for the different non local parameters via two different viscous parameter $\beta = 0.3$ and $\beta = 0.5$. The values of non-dimensional pulsation frequency decreases from higher frequency to the lower one with rising $e_0 a / l$ and with in the higher range of non-dimensional pulsation amplitude the trend is reversed.
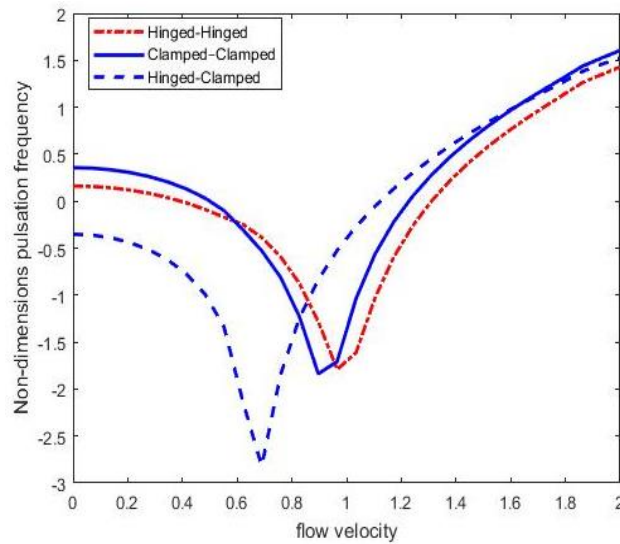
Fig. 6 Distributions of non-dimensions pulsation frequency versus flow velocity via different boundary conditions with $k_n = 0.001 \& \beta = 0.3$
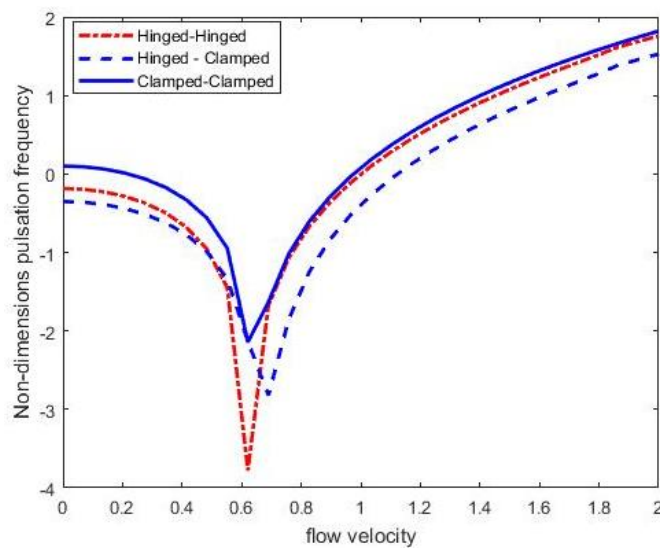


Fig. 7 Distributions of non-dimensions pulsation frequency versus flow velocity via different boundary conditions with $k_n = 0.01 \& \beta = 0.5$

More over, the influence of non local and viscous effct is more in larger values of non dimensional pulsation frequency which leads to the enhanced stability of viscous fluid conveying CNT. Figs. 4 and 5 shows the distribution of non-dimensional pulsation frequency of fluid conveying CNT against non-dimensional pulsation amplitude for various Knudsen number via $\beta = 0.3$ and $\beta = 0.5$. From the Figs. 4 and 5, it is noticed that, the non-dimensional pulsation frequency displacement rises towards positive values as non-dimensional pulsation amplitude increases for various viscous parameter and also, the rising Knudsen number reducing the pulsation frequency
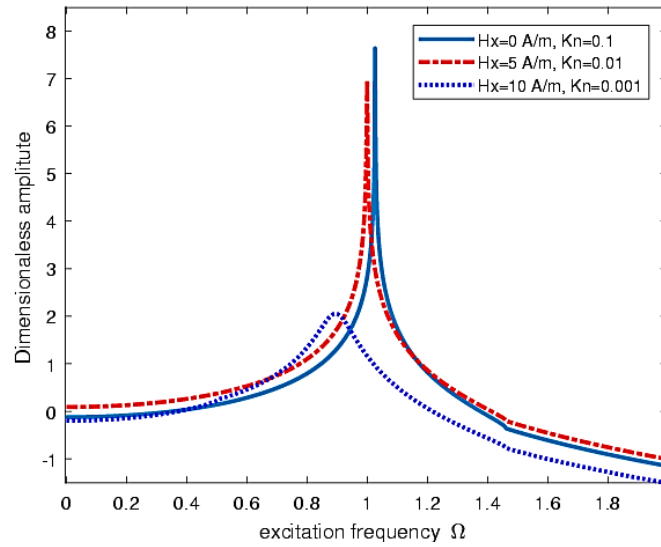
Fig. 8 Distributions of non-dimensional amplitute versus excitation frequency with $k_n = 0.01 \& \beta = 0.5$
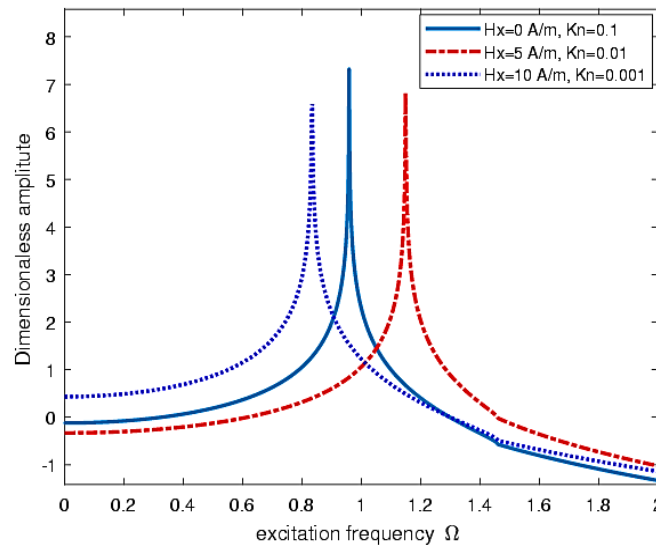


Fig. 9 Distributions of non-dimensional amplitute versus excitation frequency with $k_n = 0.01 \& \beta = 1.0$

for both the case of viscous parameter.

Figs. 6 and 7 demonstrates the variation of the non-dimensional pulsation frequency against flow velocity for the Hinged-Hinged, Clamped-Clamped and Hinged-Clamped boundaries of fluid conveying CNT with different $k_n \& \beta$ values. Here, the wave propagation is vanishing from the positive values in the lower period of flow velocity and return to rise in the higher range of flow velocity in the three boundaries. But, the wave trend is experiencing crossing over nature in the amplified values of $k_n \& \beta$ in Fig. 7.
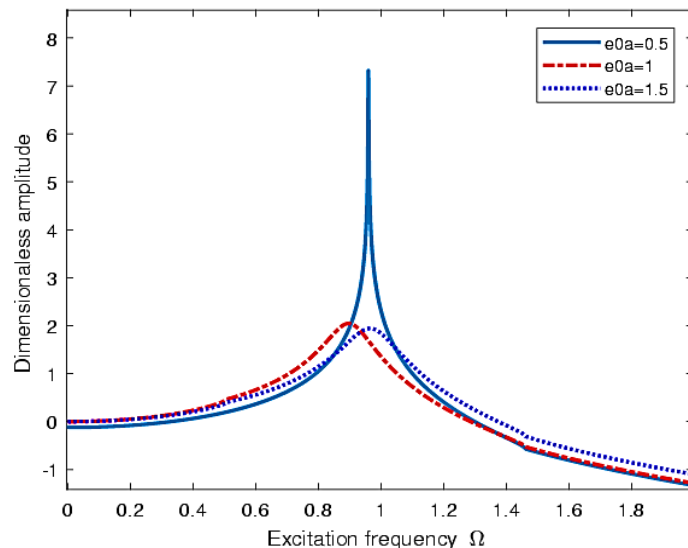
Fig. 10 Distributions of non-dimensional ampplitute versus excitation frequency with $k_n = 0.01 \& \beta = 0.5$
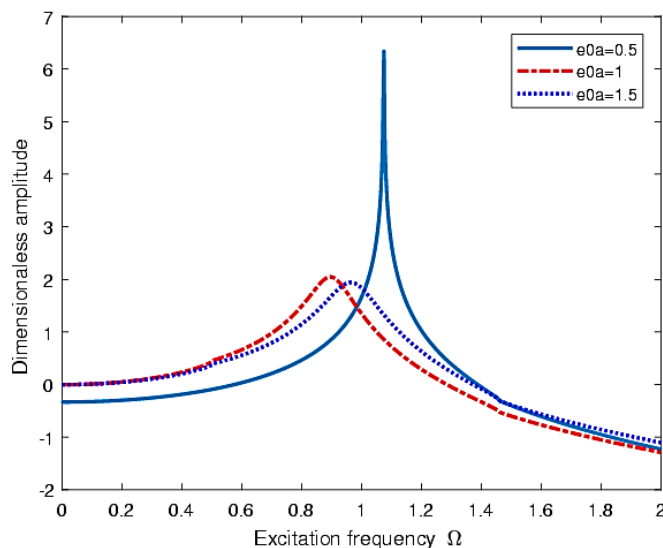


Fig. 11 Distributions of non-dimensional amplitute versus excitation frequency with $k_n = 0.01 \& \beta = 1.0$

In Figs. 8-9, the variation of dimensionless amplitude against excitation frequency with different types of magnetic flux via various viscous parameter $\beta = 0.3$ and $\beta = 0.5$ has been explored. The raise in excitation frequency results amplification in dimensionless amplitude until it attains to the resonance frequency, afterward, the dimensionless frequency will get damped. Also, the dimensionless amplitude gets higher value in higher values of Knudsen number and lower magnetic flux. Figs. 10-11, studies the variation of dimensionless amplitude against excitation frequency with different types of nonlocal parameters via various viscous parameter $\beta = 0.3$ and

$$\beta = 0.3$$
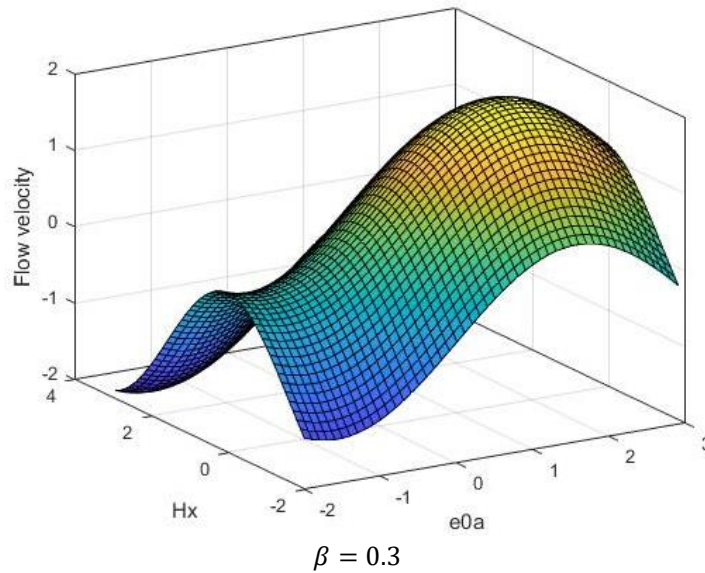
Fig. 12 3D Distributions of flow velocity via $e_0 a$ and $H_x$ with $k_n = 0.001$



$$\beta = 0.5$$
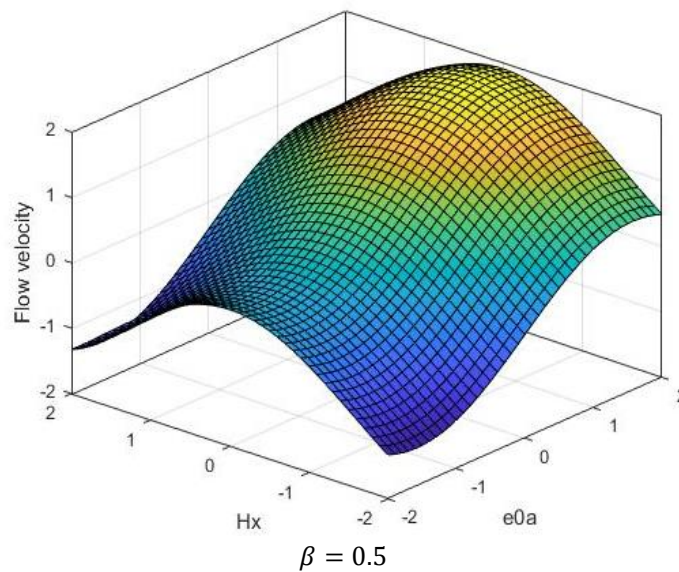
Fig. 13 3D Distributions of flow velocity via $e_0 a$ and $H_x$ with $k_n = 0.01$

$\beta = 0.5$. The raise in excitation frequency shows the same trend as in magnetic flux, but raise in non-local parameter weakens the dimensionless amplitude. Also, it is noticeable that, the resonance frequency is $\Omega \sim 1$.

The 3D curves display the physical variant non dimensional pulsation frequency and flow velocity of fluid conveying CNT with both magnetic flux and nonlocal values $H_x \& e0a$ via various $k_n \& \beta$. These figures manifests the dependence of the non-dimensional pulsation frequency and flow velocity with the driving physical constants.

$$\beta = 0.3$$
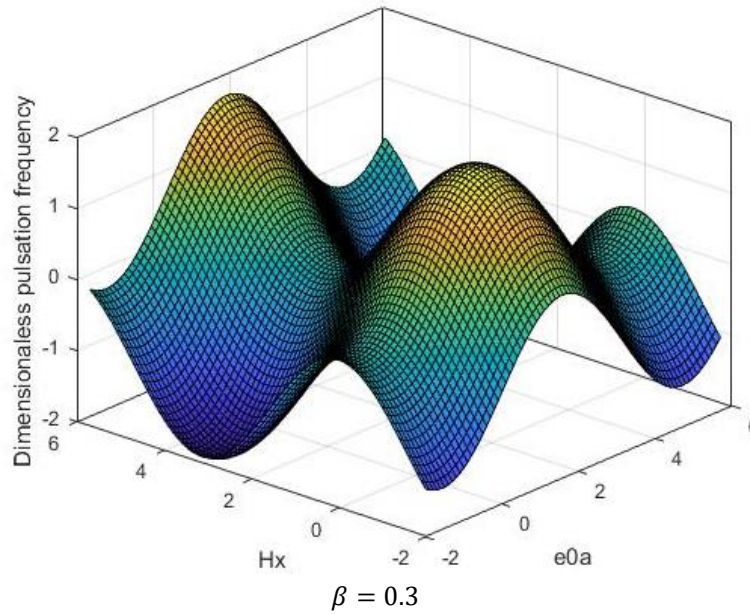
Fig. 15 3D Distributions of dimensionless pulsation frequency via $e_0 a$ and $H_x$ with $k_n = 0.01$

## 6. Conclusions

Presented paper was developed to expose a reliable and efficient mathematical analytical model and solution of dispersion equation for the vibration of thermo elastic carbon nanotubes conveying pulsating viscous nano fluid subjected to a longitudinal magnetic field via Euler-Bernoulli beam model. The controlling partial differential equation of motion is arrived by adopting Eringen's non local theory. The pulsation frequency of the CNT is obtained through the Galerkin's method. The numerical evaluation of this study is devised by Haar wavelet method (HWM). Then, the proposed model is validated by analysing the critical buckling load computed in present study with the literature and good consistency is reached. Finally, the numerical calculation of system parameters are shown as dispersion graphs and tables over non local parameter, magnetic flux, Knudsen number and viscous parameter. Based on the simulation results, the conclusions are as follows:

• The values of non-dimensional pulsation frequency decreases from higher frequency to the lower one with rising non local parameter and with in the higher range of non-dimensional pulsation amplitude the trend is reversed.
• The non-dimensional pulsation frequency rises when increases the viscous parameter and reducing its magnitude while rising Knudsen number.
• The flow velocity attains higher amplitude in lower temperature difference and receives higher dynamic responses in increasing viscous parameter and Knudsen number.
• The increase of magnetic flux results amplification in the non-dimensional pulsation frequency. Also, the C-C boundary achieves higher pulsation frequency.
• It is clear that increasing in excitation frequency causes a normalized amplitude variation in all kind of physical variants.

# References

Amiri, A., Talebitooti, R. and Li, L. (2018), "Wave propogation is viscous-fluid-conveying piezoelectric nanotubes considering surface stress effects and Kundsen number based on nonlocal strain gradient theory", *Eur. Phys. J. Plus*, **133**, 1-17. https://doi.org/10.1140/epjp/i2018-12077-y.

Ariaratnam, S.T. and Namachchivaya, N.S. (1986), "Dynamic stability of pipes conveying pulsating fluid", *J. Sound. Vib.*, **107**(2), 215-230. https://doi.org/10.1016/0022-460X(86)90233-6.

Azrar, A., Azrar, L. and Aljinaidi, A.A. (2015), "Numerical modeling of dynamic and parametric instabilities of single-walled carbon nanotubes conveying pulsating and viscous fluid", *Compos. Struct.*, **125**, 127-143. https://doi.org/10.1016/j.compstruct.2015.01.044.

Chen, C.F. and Hsiao, C.H. (1997), "Haar wavelet method for solving lumped and distributed-parameter systems", *IEE Proc. Contr. Theor. Appl.*, **144**(1), 87-94. https://doi.org/10.1049/ip-cta:19970702.

Eringen, A.C. (1983), "On differential equation of nonlocal elasticity and solution", *J. Appl. Phys.*, **54**, 4703-4710. https://doi.org/10.1063/1.332803.

Eringen, A.C. and Edelen, D.G.B. (1972), "On nonlocal elasticity", *Int. J. Eng. Sci.*, **10**, 233-248. https://doi.org/10.1016/0020-7225(72)90039-0.

Ghavanloo, E. and Fazelzadeh, S.A. (2011), "Flow-thermoelastic vibration and instability analysis of viscoelastic carbon nanotubes embedded in viscous fluid", *Physica E: Low Dimens. Syst. Nanostruct.*, **44**, 17-24. https://doi.org/10.1016/j.physe.2011.06.024.

Ghavanloo, E., Rafiei, M. and Daneshman, F. (2011), "In-plane vibration analysis of curved carbon nanotubes conveying fluid embedded in viscoelastic medium", *Phys. Lett. A.*, **375**, 1994-1999. https://doi.org/10.1016/j.physleta.2011.03.025.

Güven, U. (2014), Transverse vibrations of single-walled carbon nanotubes with initial stress under magnetic field", *Compos. Struct.*, **114**, 92-98. https://doi.org/10.1016/j.compstruct.2014.03.054.

Hajdo, E., Mejia-Nava, R.A., Imamovic, I. and Ibrahimbegovic, A. (2021), "Linearized instability analysis of frame structures under non-conservative loads: Static and dynamic approach", *Couple. Syst. Mech.*, **10**(1), 79-102. https://doi.org/10.12989/csm.2021.10.1.079.

Hariharan, G. and Kannan, K. (2014), "Review of wavelet methods for the solution of reaction-diffusion problems in science and Engineering", *Appl. Math. Model.*, **38**(3), 799-813. https://doi.org/10.1016/j.apm.2013.08.003.

Hein, H. and Feklistova, L. (2011), "Computationally eflcient delamination detection in composite beams using Haar wavelets", *Mech. Syst. Signal. Pr.*, **25**(6), 2257-2270. https://doi.org/10.1016/j.ymssp.2011.02.003.

Heydari, M.H., Hooshmandasl, M.R., Mohammadi, F. and Cattani, C. (2014), "Wavelets method for solving systems of nonlinear singular fractional Volterraintegro-differential equations", *Commun. Nonlin. Sci. Numer. Simul.*, **19**(1), 37-48. https://doi.org/10.1016/j.cnsns.2013.04.026.

Hosseini, M. and Sadeghi-Goughari, M. (2016), "Vibration and instability analysis of nanotubes conveying fluid subjected to a longitudinal magnetic field", *Appl. Math. Model.*, **40**, 2560-2576. https://doi.org/10.1016/j.apm.2015.09.106.

Hsiao, C.H. (2015), "A Haar wavelets method of solving differential equations characterizing the dynamics of a current collection system for an electric locomotive", *Appl. Math. Comput.*, **265**, 928-935. https://doi.org/10.1016/j.amc.2015.06.007.

Ibrahimbegovic, A. and Mejia-Nava, R.A. (2021), "Heterogeneities and material-scales providing physically-based damping to replace Rayleigh damping for any structure size", *Couple. Syst. Mech.*, **10**(3), 201-216. https://doi.org/10.12989/csm.2021.10.3.201.

Ibrahimbegovic, A., Mejia-Nava, R.A., Hajdo, E. and Limnios, N. (2022), "Instability of (heterogeneous) Euler beam: Deterministic vs. stochastic reduced model approach", *Couple. Syst. Mech.*, **11**(2), 167-198. https://doi.org/10.12989/csm.2022.11.2.167.

Jena, S.K. and Chakraverty, S. (2019), "Dynamic behavior of an electromagnetic nanobeam using theHaar wavelet method and the higher-order Haar wavelet method", *Eur. Phys. J. Plus*, **134**, 1-18.

https://doi.org/10.1140/epjp/i2019-12874-8.

Jena, S.K., Chakraverty, S. and Malikan, M. (2019), "Implementation of Haar wavelet, higher order Haar wavelet, and differential quadrature methods on buckling response of strain gradient nonlocal beam embedded in an elastic medium", *Eng. Comput.*, https://doi.org/10.1007/s00366-019-00883-1.

Jin, G., Xie, X. and Liu, Z. (2013), "Free vibration analysis of cylindrical shells using the Haar wavelet method", *Int. J. Mech. Sci.*, **77**, 47-56. https://doi.org/10.1016/j.ijmecsci.2013.09.025.

Jin, G., Xie, X. and Liu, Z. (2014), "The Haar wavelet method for free vibration analysis of functionally graded cylindrical shells based on the shear deformation theory", *Compos. Struct.*, **108**, 435-448. https://doi.org/10.1016/j.compstruct.2013.09.044.

Jin, J.D. and Song, Z.Y. (2005), "Parametric resonances of supported pipes conveying pulsating fluid", *J. Fluid. Struct.*, **20**(6), 763-783. https://doi.org/10.1016/j.jfluidstructs.2005.04.007.

Karličić, D., Kozić, P., Pavlović, R. and Nešić, N. (2017), "Dynamic stability of single-walled carbon nanotube embedded in a viscoelastic medium under the influence of the axially harmonic load", *Compos. Struct.*, **162**, 227-243. https://doi.org/10.1016/j.compstruct.2016.12.003.

Kiani, K. (2014), "Vibration and instability of a single-walled carbon nanotube in a three-dimensional magnetic field", *J. Phys. Chem. Solid.*, **75**, 15-22. https://doi.org/10.1016/j.jpcs.2013.07.022.

Kiani, K. (2015), "Stability and vibrations of doubly parallel current carrying nanowires immersed in a longitudinal magnetic field", *Phys. Lett. A*, **379**, 348-360. https://doi.org/10.1016/j.physleta.2014.11.006.

Kuang, Y.D., He, X.Q., Chen, C.Y. and Li, G.Q. (2009), "Analysis of nonlinear vibrations of double-walled carbon nanotubes conveying fluid", *Comput. Mater. Sci.*, **45**, 875-880. https://doi.org/10.1016/j.commatsci.2008.12.007.

Lee, H.L. and Chang, W.J. (2008), "Free transverse vibration of the fluid-conveying single-walled carbon nanotube using nonlocal elastic theory", *J. Appl. Phys.*, **103**, 024302-024305. https://doi.org/10.1063/1.2822099.

Lei, X.W., Natsuki, T., Shi, J.X. and Ni, Q.Q. (2012), "Surface effects on the vibrational frequency of double-walled carbon nanotubes using the nonlocal Timoshenko beam model", *Compos. B. Eng.*, **43**, 64-69. https://doi.org/10.1016/j.compositesb.2011.04.032.

Lepik, Ü. (2011), "Buckling of elastic beams by the Haar wavelet method", *Estonian J. Eng.*, **17**, 271.

Li, L., Hu, Y. and Ling, L. (2016), "Wave propagation in viscoelastic single-walled carbon nanotubes with surface effect under magnetic field based on nonlocal strain gradient theory", *Physica E: Low Dimens. Syst. Nanostruct.*, **75**, 118-124. https://doi.org/10.1016/j.physe.2015.09.028.

Liu, H., Liu, Y., Dai, J. and Cheng, Q. (2018), "An improved model of carbon nanotube conveying flow by considering comprehensive effects of Knudsen number", *Microfluid Nanofluidics.*, **22**, 66. https://doi.org/10.1007/s10404-018-2088-7.

Mahaveer Sree Jayan, M., Kumar, R., Selvamani, R. and Rexy, J. (2020), "Nonlocal dispersion analysis of a fluid-conveying thermo elastic armchair single walled carbon nanotube under moving harmonic excitation", *J. Solid. Mech.*, **12**(1), 189-203. https://doi.org/10.22034/JSM.2019.1867399.1431.

Murmu, T., McCarthy, M.A. and Adhikari, S. (2012), "Vibration response of double-walled carbon nanotubes subjected to an externally applied longitudinal magnetic field: A nonlocal elasticity approach", *J. Sound. Vib.*, **331**, 5069-5086. https://doi.org/10.1016/j.jsv.2012.06.005.

Nguyen, C.U., Hoang, T.V., Hadzalic, E., Dobrilla, S., Matthies, H.G. and Ibrahimbegovic, A. (2022), "Viscoplasticity model stochastic parameter identification: Multi-scale approach and Bayesian inference", *Couple Syst. Mech.*, **11**(5), 411-442. https://doi.org/10.12989/csm.2022.11.5.411.

Ni, B., Sinnott, S.B., Mikulski, P.T. and Harrison, J.A. (2002), "Compression of carbon nanotubes filled with C60, CH4, or Ne: Predictions from molecular dynamics simulations", *Phys. Rev. Lett.*, **88**, 205505. https://doi.org/10.1103/PhysRevLett.88.205505.

Ni, Q., Tang, M., Wang, Y. and Wang, L. (2014), "In-plane and out-of-plane dynamics of a curved pipe conveying pulsating fluid", *Nonlin. Dyn.*, **75**(3), 603-619. https://doi.org/10.1007/s11071-013-1089-z.

Ni, Q., Zhang, Z., Wang, L., Qian, Q. and Tang, M. (2014), "Nonlinear dynamics and synchronization of two coupled pipes conveying pulsating fluid", *Acta Mechanica Solida Sinica*, **27**(2), 162-171. https://doi.org/10.1016/S0894-9166(14)60026-4.

Noah, S.T. and Hopkins, G.R. (1980), "Dynamic stability of elastically supported pipes conveying pulsating fluid", *J. Sound. Vib.*, **71**(1), 103-116. https://doi.org/10.1016/0022-460X(80)90411-3.

Paidoussis, M.P. (1998), *Fluid-Structure Interactions: Slender Structures and Axial Flow*, Vol. 1, Academic Press.

Paidoussis, M.P. and Sundararajan, C. (1975), "Parametric and combination resonances of a pipe conveying pulsating fluid", *J. Appl. Mech.*, **42**(4), 780-784. https://doi.org/10.1115/1.3423705.

Panda, L.N. and Kar, R.C. (2007), "Nonlinear dynamics of a pipe conveying pulsating fluid with parametric and internal resonances", *Nonlin. Dyn.*, **49**(1-2), 9-30. https://doi.org/10.1007/s11071-006-9100-6.

Panda, L.N. and Kar, R.C. (2008), "Nonlinear dynamics of a pipe conveying pulsating fluid with combination, principal parametric and internal resonances", *J. Sound. Vib.*, **309**(3-5), 375-406. https://doi.org/10.1016/j.jsv.2007.05.023.

Pipes, R.B. and Hubert, P. (2003), "Helical carbon nanotube arrays: Thermal expansion", *Compos. Sci. Technol.*, **63**, 1571-1579. https://doi.org/10.1016/S0266-3538(03)00075-7.

Raravikar, N.R., Keblinski, P., Rao, A.M., Dresselhaus, M.S., Schadler, L.S. and Ajayan, P.M. (2002), "Temperature dependence of radial breathing mode Raman frequency of single-walled carbon nanotubes", *Phys. Rev. B.*, **66**, 235424. https://doi.org/10.1103/PhysRevB.66.235424.

Rashidi, V., Mirdamadi, H.R. and Shiran, E. (2012), "A novel model for vibrations of nanotubes conveying nanoflow", *Comput. Mater. Sci.*, **51**, 347-352. https://doi.org/10.1016/j.commatsci.2011.07.030.

Schelling, P.K. and Keblinski, P. (2003), "Thermal expansion of carbon structures", *Phys. Rev. B.*, **68**, 035425. https://doi.org/10.1103/PhysRevB.68.035425.

Selvamani, R. and Ponnusamy, P. (2013), "Wave propagation in a generalized thermo elastic circular plate immersed in fluid", *Struct. Eng. Mech.*, **46**(6), 827-842. http://doi.org/10.12989/sem.2013.46.6.827.

Selvamani, R., Mahaveer Sree Jayan, M. and Ebrahimi, F. (2021), "Ultrasonic waves in a single walled armchair carbon nanotube resting on nonlinear foundation subjected to thermal and in plane magnetic fields", *Couple. Syst. Mech.*, **10**(1), 39-60. http://doi.org/10.12989/csm.2021.10.1.039.

Selvamani, R., Mahaveer Sree Jayan, M., Dimitri, R., Tornabene, R. and Ebrahimi, F. (2020), "Nonlinear magneto-thermo-elastic vibration of mass sensor armchair carbon nanotube resting on an elastic substrate", *Curve. Layer. Struct.*, **7**, 153-165. https://doi.org/10.1515/cls-2020-0012.

Selvamani, R., Mahesh, S. and Ebrahimi, F. (2021), "Frequency characteristics of a multiferroic Piezoelectric/LEMV/CFRP/Piezomagnetic composite hollow cylinder under the influence of rotation and hydrostatic stress", *Couple. Syst. Mech.*, **10**(2), 185. http://doi.org/10.12989/csm.2021.10.2.185.

Tokio, Y. (1995), "Recent development of carbon nanotube", *Synthetic Metal.*, **70**, 1511-1518. https://doi.org/10.1016/0379-6779(94)02939-V.

Wang, L. (2009), "Dynamical behaviors of double-walled carbon nanotubes conveying fluid accounting for the role of small length scale", *Comput. Mater. Sci.*, **45**, 584-588. https://doi.org/10.1016/j.commatsci.2008.12.006.

Wang, L. (2009), "Vibration and instability analysis of tubular nano- and micro-beams conveying fluid using nonlocal elastic theory", *Physica E: Low Dimens. Syst. Nanostruct.*, **41**, 1835-1840. https://doi.org/10.1016/j.physe.2009.07.011.

Wang, L., Ni, Q., Li, M. and Qian, Q. (2008), "The thermal effect on vibration and instability of carbon nanotubes conveying fluid", *Physica E: Low Dimens. Syst. Nanostruct.*, **40**, 3179-3182. https://doi.org/10.1016/j.physe.2008.05.009.

Xia, W. and Wang, L. (2010), "Vibration characteristics of fluid-conveying carbon nanotubes with curved longitudinal shape", *Comput. Mater. Sci.*, **49**, 99-103. https://doi.org/10.1016/j.commatsci.2010.04.030.

Zhang, C.L. and Shen, H.S. (2006), "Temperature-dependent elastic properties of single-walled carbon nanotubes: Prediction from molecular dynamics simulation", *Appl. Phys. Lett.*, **89**, 081904. https://doi.org/10.1063/1.2336622.

Zhang, D.P., Lei, Y. and Shen, Z.B. (2017), "Effect of longitudinal magnetic field on vibration characteristics of single-walled carbon nanotubes in a viscoelastic medium", *Brazil. J. Phys.*, **47**, 640-656. https://doi.org/10.1007/s13538-017-0524-x.

Zhang, Q., Yang, D.J., Wang, S.G., Yoon, S.F. and Ahn, J. (2006), "Influences of temperature on the Raman

spectra of single-walled carbon nanotubes", *Smart. Mater. Struct.*, **15**(1), S1. https://doi.org/10.1088/0964-1726/15/1/001.

Zhang, Y.C. and Wang, X. (2005), "Thermal effects on interfacial stress transfer characteristics of carbon nanotubes/polymer composites", *Int. J. Solid. Struct.*, **42**, 5399-5412. https://doi.org/10.1016/j.ijsolstr.2005.02.038.

Zhang, Y.F., Yao, M.H., Zhang, W. and Wen, B.C. (2017), "Dynamical modeling and multi-pulse chaotic dynamics of cantilevered pipe conveying pulsating fluid in parametric resonance", *Aerosp. Sci. Technol.*, **68**, 441-453. https://doi.org/10.1016/j.ast.2017.05.027.

Zhang, Y.Q., Liu, X. and Liu, G.R. (2007), "Thermal effect on transverse vibrations of double-walled carbon nanotubes", *Nanotechnol.*, **18**, 44570. https://doi.org/10.1088/0957-4484/18/44/445701.

Zhen, Y.X., Fang, B. and Tang, Y. (2011), "Thermal-mechanical vibration and instability analysis of fluid-conveying double walled carbon nanotubes embedded in visco-elastic medium", *Physica E: Low Dimens. Syst. Nanostruct.*, **44**, 379-385. https://doi.org/10.1016/j.physe.2011.09.004.

*AI*